

See discussions, stats, and author profiles for this publication at: <https://www.researchgate.net/publication/249230401>

Neutrino Energy Loss in Stellar Interiors. VII. Pair, Photo, Plasma, Bremsstrahlung, and Recombination Neutrino Processes

Article in *The Astrophysical Journal Supplement Series* · February 1996

DOI: 10.1086/192264

CITATIONS

338

READS

62

4 authors, including:



Naoki Itoh

Sophia University

58 PUBLICATIONS 1,979 CITATIONS

[SEE PROFILE](#)



Akinori Nishikawa

Wakayama Medical University

29 PUBLICATIONS 447 CITATIONS

[SEE PROFILE](#)

NEUTRINO ENERGY LOSS IN STELLAR INTERIORS. VII. PAIR, PHOTO-, PLASMA, BREMSSTRAHLUNG, AND RECOMBINATION NEUTRINO PROCESSES

NAOKI ITOH, HIROSHI HAYASHI, AND AKINORI NISHIKAWA
 Department of Physics, Sophia University, 7-1 Kioi-cho, Chiyoda-ku, Tokyo, 102, Japan

AND

YASU HARU KOHYAMA
 Fuji Research Institute Corporation, 3-18-1 Kaigan, Minato-ku, Tokyo, 108, Japan
Received 1995 January 3; accepted 1995 July 27

ABSTRACT

The results of the calculations of the neutrino energy-loss rates resulting from pair, photo-, plasma, bremsstrahlung, and recombination neutrino processes are summarized in the form of analytic fitting formulae and tables. Care has been taken in order to serve the convenience of the users of these results. We have tried to make the present paper as self-contained as possible. The contents of the present paper are intended to serve as useful physical input data for stellar evolution computations. We intend to publish the numerical data and the FORTRAN codes for the results of the neutrino energy-loss rates in the CD-ROM series of the American Astronomical Society. In the CD-ROM, we intend to give three options for the FORTRAN codes. The first option comprises the results with analytic fitting formulae only. The second option comprises the results with analytic fitting formulae for the bremsstrahlung and recombination neutrino processes, and the numerical tables for the pair, photo-, and plasma neutrino processes with a standard quadratic interpolation procedure. In this option, the grid of $\log T$ for the pair neutrino energy-loss rate is 0.2. The third option is a variant of the second option, with the replacement of the grid of $\log T$ for the pair neutrino energy-loss rate to be 0.05.

Subject headings: dense matter — elementary particles — methods: numerical — radiation mechanisms: nonthermal — stars: interiors

1. INTRODUCTION

In the past decade, two of the present authors (N. I. and Y. K.), together with their collaborators, have systematically investigated the neutrino energy loss in stellar interiors based on the Weinberg-Salam theory (Itoh & Kohyama 1983; Itoh et al. 1984a, b, c; Munakata, Kohyama, & Itoh 1985; Kohyama, Itoh, & Munakata 1986; Munakata, Kohyama, & Itoh 1987; Itoh et al. 1989, 1992; Kohyama et al. 1993, 1994). They have dealt with the pair, photo-, plasma, bremsstrahlung, and recombination neutrino processes. Dicus (1973), Dicus et al. (1976), Schinder et al. (1987), Braaten (1991), Braaten & Segel (1993), and Haft, Raffelt, & Weiss (1994) also calculated the neutrino energy-loss rates using the Weinberg-Salam theory. The calculations of the neutrino energy-loss rates based on the Feynman-Gell-Mann theory were summarized by Beaudet, Petrosian, & Salpeter (1967).

In 1989 Itoh et al. (1989) summarized the calculations of the neutrino energy loss rates attributable to the pair, photo-, plasma, and bremsstrahlung processes. However, major improvements on the numerical result of the plasma neutrino energy-loss rates have recently become available (Braaten 1991; Itoh et al. 1992; Braaten & Segel 1993; Kohyama et al. 1994). The neutrino energy-loss rates resulting from the recombination process have also been accurately calculated very recently (Kohyama et al. 1993). Therefore, it is useful to summarize the results of the neutrino energy-loss rates resulting from the pair, photo-, plasma, bremsstrahlung, and recombination processes and to update the results of Itoh et al. (1989). In this

paper we take care to serve the convenience of the users of the results of the neutrino energy-loss rates. For that purpose, we present analytic fitting formulae and numerical tables. We try to make the present paper as self-contained as possible. The contents of the present paper are intended to serve as useful physical input data for stellar evolution computations. We plan to publish the numerical data and the FORTRAN codes for the results of the neutrino energy-loss rates in the CD-ROM series of the American Astronomical Society.

The bremsstrahlung neutrino process essentially depends on the states of ions. Therefore, different methods must be applied to the calculations of the neutrino energy-loss rates corresponding to different regimes of densities and temperatures. Thus, analytic fitting formulae are best suited to express the numerical results of the bremsstrahlung neutrino process. The results of the recombination neutrino process can be expressed in a semianalytical way. Therefore, analytic fitting formulae are also best suited to express the numerical results of this process.

Regarding the expression of the numerical results of pair, photo-, and plasma neutrino energy-loss rates, in the accompanying CD-ROM version, we give three options. The first option uses analytical fitting formulae for these three processes. The accuracy of the fitting formulae is generally better than 10% where the respective neutrino process is the most dominant process. We will describe the accuracy and the validity region of the fitting formulae in more detail when we describe the explicit forms of the fitting formulae. The reason why we give this option of the analytical fitting formulae is that this is

efficient and time-saving, although the accuracy may not be too high in some density-temperature regions. For those who do not wish their neutrino-loss subroutine to become too heavy, we recommend this option. It is our belief that for ordinary stellar evolution computations which do not require higher accuracy than 10% for the neutrino energy-loss rates, this option should be sufficient.

The second option comprises the numerical tables for the pair, photo-, and plasma neutrino processes with a standard quadratic interpolation procedure. In this option, the grid of $\log T$ for the pair neutrino energy-loss rate is 0.2. The third option is a variant of the second option, with the replacement of the grid of $\log T$ for the pair neutrino energy-loss rate to be 0.05. Users who require higher accuracies for the neutrino energy-loss rates may use these options according to their choice of the burdens of the neutrino-loss subroutine.

The present paper is organized as follows. The pair neutrino process is summarized in § 2. The photoneutrino process is summarized in § 3. The plasma neutrino process is summarized in § 4. The bremsstrahlung neutrino process is summarized in § 5. The recombination neutrino process is summarized in § 6. Comparison of various neutrino processes is made in § 7. Concluding remarks are given in § 8.

2. PAIR NEUTRINO PROCESS

In this paper we report on the results of the calculations of the neutrino energy loss-rates based on the Weinberg-Salam theory (Weinberg 1967; Salam 1968). The energy-loss rate resulting from the pair neutrino process is expressed as (Munakata et al. 1985; Itoh et al. 1989)

$$Q_{\text{pair}} = \frac{1}{2}[(C_V^2 + C_A^2) + n(C_V'^2 + C_A'^2)]Q_{\text{pair}}^+ + \frac{1}{2}[(C_V^2 - C_A^2) + n(C_V'^2 - C_A'^2)]Q_{\text{pair}}^-, \quad (2.1)$$

$$C_V = \frac{1}{2} + 2 \sin^2 \theta_W, \quad C_A = \frac{1}{2}, \quad (2.2)$$

$$C_V' = 1 - C_V, \quad C_A' = 1 - C_A, \quad (2.3)$$

$$\sin^2 \theta_W = 0.2319 \pm 0.0005, \quad (2.4)$$

where θ_W is the Weinberg angle and n is the number of the neutrino flavors other than the electron neutrino whose masses can be neglected compared with $k_B T$. In this paper, we employ the most recent value of the Weinberg angle.

Itoh et al. (1989) calculated the pair neutrino energy-loss rates for the density-temperature region $10^0 \leq \rho/\mu_e (\text{g cm}^{-3}) \leq 10^{14}$, $10^7 \leq T(\text{K}) \leq 10^{11}$, and presented an accurate analytic fitting formula. In the CD-ROM version, we show the numerical tables of Q_{pair}^+ and Q_{pair}^- in equation (2.1).

We show the analytic fitting formula of Itoh et al. (1989) for the pair neutrino process (the numerical results for the neu-

trino energy-loss rates are expressed in units of $\text{ergs cm}^{-3} \text{s}^{-1}$ throughout the present paper, unless stated otherwise):

$$Q_{\text{pair}} = \frac{1}{2}[(C_V^2 + C_A^2) + n(C_V'^2 + C_A'^2)] \times \left[1 + \frac{(C_V^2 - C_A^2) + n(C_V'^2 - C_A'^2)}{(C_V^2 + C_A^2) + n(C_V'^2 + C_A'^2)} q_{\text{pair}} \right] \times g(\lambda) e^{-2/\lambda} f_{\text{pair}}, \quad (2.5)$$

$$q_{\text{pair}} = (10.7480\lambda^2 + 0.3967\lambda^{0.5} + 1.0050)^{-1.0} \times [1 + (\rho/\mu_e)(7.692 \times 10^7 \lambda^3 + 9.715 \times 10^6 \lambda^{0.5})^{-1.0}]^{-0.3}, \quad (2.6)$$

$$f_{\text{pair}} = \frac{(a_0 + a_1 \xi + a_2 \xi^2) e^{-c\xi}}{\xi^3 + b_1 \lambda^{-1} + b_2 \lambda^{-2} + b_3 \lambda^{-3}}, \quad (2.7)$$

$$g(\lambda) = 1 - 13.04\lambda^2 + 133.5\lambda^4 + 1534\lambda^6 + 918.6\lambda^8, \quad (2.8)$$

$$\xi = \left(\frac{\rho/\mu_e}{10^9 \text{ g cm}^{-3}} \right)^{1/3} \lambda^{-1}, \quad (2.9)$$

$$\lambda = \frac{T}{5.9302 \times 10^9 \text{ K}}, \quad (2.10)$$

where ρ/μ_e is measured in units of g cm^{-3} .

The numerical values of the coefficients a_i , b_j , and c are presented in Table 1. The accuracy of the fitting is generally better than about 10% when the pair neutrino process is the most dominant process. The accuracy of the fitting becomes poor in the region in which the relative importance of the pair neutrino process decreases. In particular, at higher densities at which the pair neutrino energy-loss rate starts to decline, the accuracy also sometimes decreases to $\sim 50\%$. When users are concerned with these regions, we recommend using the numerical tables instead. Apart from these regions, the analytical fitting formulae are considered to be useful. The fitting formulae are prescribed so that they generally give values which are smaller than the exact values when these two differ considerably. Thus, the use of the fitting formulae will not introduce errors of any significance. The reader is referred to the figures of this paper in order to compare the relative importance of various neutrino processes.

3. PHOTONEUTRINO PROCESS

The energy-loss rate resulting from the photoneutrino process is expressed as (Munakata et al. 1985; Itoh et al. 1989)

$$Q_{\text{photo}} = \frac{1}{2}[(C_V^2 + C_A^2) + n(C_V'^2 + C_A'^2)]Q_{\text{photo}}^+ - \frac{1}{2}[(C_V^2 - C_A^2) + n(C_V'^2 - C_A'^2)]Q_{\text{photo}}^-. \quad (3.1)$$

TABLE 1

NUMERICAL VALUES FOR COEFFICIENTS OF THE PAIR NEUTRINO FITTING FORMULA

$T(\text{K})$	a_0	a_1	a_2	b_1	b_2	b_3	c
$< 10^{10}$	6.002E+19	2.084E+20	1.872E+21	9.383E-1	-4.141E-1	5.829E-2	5.5924
$> 10^{10}$	6.002E+19	2.084E+20	1.872E+21	1.2383	-0.8141	0.0	4.9924

Itoh et al. (1989) calculated the photoneutrino energy-loss rates for the density-temperature region $10^0 \leq \rho/\mu_e$ (g cm^{-3}) $\leq 10^{11}$, $10^7 \leq T(\text{K}) \leq 10^{11}$, and they presented a table of the numerical results and an accurate analytic fitting formula. Their results supersede those of Munakata et al. (1985) and Schinder et al. (1987). In the CD-ROM version, we present the numerical tables of Q_{photo}^+ and Q_{photo}^- in equation (3.1).

We present the fitting formula of Itoh et al. (1989) for the photoneutrino process:

$$Q_{\text{photo}} = \frac{1}{2} [(C_V^2 + C_A^2) + n(C_V'^2 + C_A'^2)] \times \left[1 - \frac{(C_V^2 - C_A^2) + n(C_V'^2 - C_A'^2)}{(C_V^2 + C_A^2) + n(C_V'^2 + C_A'^2)} q_{\text{photo}} \right] \times \left(\frac{\rho}{\mu_e} \right) \lambda^5 f_{\text{photo}}, \quad (3.2)$$

$$q_{\text{photo}} = 0.666(1 + 2.045\lambda)^{-2.066} \times [1 + (\rho/\mu_e)(1.875 \times 10^8 \lambda + 1.653 \times 10^8 \lambda^2 + 8.499 \times 10^8 \lambda^3 - 1.604 \times 10^8 \lambda^4)^{-1.0}]^{-1.0}, \quad (3.3)$$

$$f_{\text{photo}} = \frac{(a_0 + a_1 \xi + a_2 \xi^2) e^{-c\xi}}{\xi^3 + b_1 \lambda^{-1} + b_2 \lambda^{-2} + b_3 \lambda^{-3}}. \quad (3.4)$$

$$b_1 = 6.290 \times 10^{-3}, \quad b_2 = 7.483 \times 10^{-3}, \quad b_3 = 3.061 \times 10^{-4}, \quad (3.5)$$

$$c = \begin{cases} 0.5654 + \log_{10}(T/10^7 \text{ K}) & \text{for } 10^7 \leq T(\text{K}) < 10^8, \\ 1.5654 & \text{for } 10^8 \leq T(\text{K}), \end{cases} \quad (3.6)$$

$$a_i = \frac{1}{2} c_{i0} + \sum_{j=1}^5 [c_{ij} \cos(\frac{5}{3} \pi j \tau) + d_{ij} \sin(\frac{5}{3} \pi j \tau)] + \frac{1}{2} c_{i6} \cos(10\pi\tau) \quad (i = 0, 1, 2), \quad (3.7)$$

$$\tau = \begin{cases} \log_{10}(T/10^7 \text{ K}) & \text{for } 10^7 \leq T(\text{K}) < 10^8, \\ \log_{10}(T/10^8 \text{ K}) & \text{for } 10^8 \leq T(\text{K}) < 10^9, \\ \log_{10}(T/10^9 \text{ K}) & \text{for } 10^9 \leq T(\text{K}). \end{cases} \quad (3.8)$$

The numerical values of the coefficients c_{ij} and d_{ij} are presented in Table 2. The accuracy of the fitting formula is about 1% in most of the region in which the photoneutrino process dominates over the other processes. However, we caution that the accuracy of the fitting formula deteriorates rapidly outside this region. For those who wish to calculate the photoneutrino energy-loss rates in the density-temperature region in which the photoneutrino process is not the most dominant process, we

TABLE 2
NUMERICAL VALUES FOR COEFFICIENTS OF THE PHOTONEUTRINO FITTING FORMULA

A. VALUES OF c_{ij}							
i	j						
	0	1	2	3	4	5	6
$10^7 \leq T(\text{K}) < 10^8$							
0.....	1.008E+11	0	0	0	0	0	0
1.....	8.156E+10	9.728E+8	-3.806E+9	-4.384E+9	-5.774E+9	-5.249E+9	-5.153E+9
2.....	1.067E+11	-9.782E+9	-7.193E+9	-6.936E+9	-6.893E+9	-7.041E+9	-7.193E+9
$10^8 \leq T(\text{K}) < 10^9$							
0.....	9.889E+10	-4.524E+8	-6.088E+6	4.269E+7	5.172E+7	4.910E+7	4.388E+7
1.....	1.813E+11	-7.556E+9	-3.304E+9	-1.031E+9	-1.764E+9	-1.851E+9	-1.928E+9
2.....	9.750E+10	3.484E+10	5.199E+9	-1.695E+9	-2.865E+9	-3.395E+9	-3.418E+9
$10^9 \leq T(\text{K})$							
0.....	9.581E+10	4.107E+8	2.305E+8	2.236E+8	1.580E+8	2.165E+8	1.721E+8
1.....	1.459E+12	1.314E+11	-1.169E+11	-1.765E+11	-1.867E+11	-1.983E+11	-1.896E+11
2.....	2.424E+11	-3.669E+9	-8.691E+9	-7.967E+9	-7.932E+9	-7.987E+9	-8.333E+9
B. VALUES OF d_{ij}							
i	j						
	1	2	3	4	5		
$10^7 \leq T(\text{K}) < 10^8$							
0.....	0	0	0	0	0		
1.....	-1.879E+10	-9.667E+9	-5.602E+9	-3.370E+9	-1.825E+9		
2.....	-2.919E+10	-1.185E+10	-7.270E+9	-4.222E+9	-1.560E+9		
$10^8 \leq T(\text{K}) < 10^9$							
0.....	-1.135E+8	1.256E+8	5.149E+7	3.436E+7	1.005E+7		
1.....	1.652E+9	-3.119E+9	-1.839E+9	-1.458E+9	-8.956E+8		
2.....	-1.548E+10	-9.338E+9	-5.899E+9	-3.035E+9	-1.598E+9		
$10^9 \leq T(\text{K})$							
0.....	4.724E+8	2.976E+8	2.242E+8	7.937E+7	4.859E+7		
1.....	-7.094E+11	-3.697E+11	-2.189E+11	-1.273E+11	-5.705E+10		
2.....	-2.254E+10	-1.551E+10	-7.793E+9	-4.489E+9	-2.185E+9		

recommend using the numerical tables instead. The fitting formulae are prescribed so that they do not give values which are larger than the correct values when the two differ considerably. Thus, the use of the fitting formulae will not introduce errors of any significance.

4. PLASMA NEUTRINO PROCESS

Kohyama et al. (1986, 1994) have shown that the axial-vector contribution to the plasma neutrino energy-loss rates is at most on the order of 10^{-4} of the vector contribution for $T \leq 10^{11}$ K. Thus, one can safely neglect the axial-vector contribution to the plasma neutrino energy-loss rates. Therefore, the plasma neutrino energy-loss rates are written as

$$Q_{\text{plasma}} = (C_V^2 + nC_V'^2)Q_V, \quad (4.1)$$

$$Q_V = Q_L + Q_T, \quad (4.2)$$

where Q_L and Q_T are the contributions of the longitudinal plasmon and the transverse plasmon, respectively.

Braaten (1991) has pointed out that the use of fully relativistic plasmon dispersion relations are indispensable for the accurate calculation of the plasma neutrino energy-loss rates. Itoh et al. (1992) have calculated the plasma neutrino energy-loss rates for the case of strongly degenerate electrons using the fully relativistic dielectric functions derived by Jancovici (1962), thereby showing that the exact calculation leads to a neutrino energy-loss rate which differs from the old result (Itoh et al. 1989) by a factor as large as 3. Itoh et al. (1989) have shown that the plasma neutrino process is the dominant process when electrons are strongly degenerate. Haft et al. (1994) calculated the plasma neutrino energy loss using the approximate formulae for the polarization functions derived by Braaten & Segel (1993). In the CD-ROM version, we show the numerical tables of Q_L and Q_T in equation (4.2) (calculated with the use of the Jancovici formulae) which are valid well below the electron Fermi temperature

$$T \ll T_F = 5.9302 \times 10^9 \{ [1 + 1.018(\rho_6/\mu_e)^{2/3}]^{1/2} - 1 \} [\text{K}], \quad (4.3)$$

$$\mu_e = \frac{A}{Z}, \quad (4.4)$$

where Z and A are the atomic number and mass number of the nucleus considered, and ρ_6 is the mass density in units of 10^6 g cm^{-3} .

Instead of using the analytic fitting formula of Itoh et al. (1992), we will reproduce here equations (23)–(27) of Haft et al. (1994). The formula reads as

$$Q_V = 3.00 \times 10^{21} \lambda^9 \gamma^6 e^{-\gamma} (f_T + f_L) f_{xy}, \quad (4.5)$$

$$\gamma^2 = \frac{1.1095 \times 10^{11} \rho / \mu_e}{T^2 [1 + (1.019 \times 10^{-6} \rho / \mu_e)^{2/3}]^{1/2}}, \quad (4.6)$$

$$f_T = 2.4 + 0.6\gamma^{1/2} + 0.51\gamma + 1.25\gamma^{3/2}, \quad (4.7)$$

$$f_L = \frac{8.6\gamma^2 + 1.35\gamma^{7/2}}{225 - 17\gamma + \gamma^2}, \quad (4.8)$$

$$x = \frac{1}{6} [17.5 + \log_{10}(2\rho/\mu_e) - 3 \log_{10} T], \quad (4.9)$$

$$y = \frac{1}{6} [-24.5 + \log_{10}(2\rho/\mu_e) + 3 \log_{10} T]. \quad (4.10)$$

If $|x| > 0.7$ or $y < 0$, we set $f_{xy} = 1$, and otherwise

$$f_{xy} = 1.05 + \{ 0.39 - 1.25x - 0.35 \sin(4.5x) - 0.3 \exp[-(4.5x + 0.9)^2] \} \times \exp \left\{ - \left[\frac{\min(0, y - 1.6 + 1.25x)}{0.57 - 0.25x} \right]^2 \right\}. \quad (4.11)$$

The accuracy of the fitting formula is better than about 5% when the plasma neutrino process is the most dominant neutrino process.

5. BREMSSTRAHLUNG NEUTRINO PROCESS

The energy-loss rates caused by the bremsstrahlung neutrino process based on the Weinberg-Salam theory have been calculated by Itoh & Kohyama (1983), Itoh et al. (1984a, b, c), and Munakata et al. (1987). Their results supersede those of Dicus et al. (1976) through the accurate inclusion of the ionic correlation effects and the screening effects attributable to electrons.

The relevant density-temperature region for the bremsstrahlung neutrino process is divided as follows. First of all, we divide the density-temperature region into two by the line $T = 0.3T_F$. When $T > 0.3T_F$, we define that the electrons are weakly degenerate. When $T < 0.3T_F$, we define that the electrons are strongly degenerate. For $T > 0.3T_F$, we use the results of the calculation of Munakata et al. (1987). (For ^4He matter, the dividing temperature is taken as $0.01T_F$.)

5.1. Weakly Degenerate Electrons

The energy loss resulting from the bremsstrahlung neutrino process for weakly degenerate electrons per unit volume per unit time is written as (we use the subscript “gas” to designate gaseous ions)

$$Q_{\text{gas}} = 0.5738 (\text{ergs cm}^{-3} \text{ s}^{-1}) (Z^2/A) T_8^6 \rho \times \left\{ \frac{1}{2} [(C_V^2 + C_A^2) + n(C_V'^2 + C_A'^2)] F_{\text{gas}} - \frac{1}{2} [(C_V^2 - C_A^2) + n(C_V'^2 - C_A'^2)] G_{\text{gas}} \right\}, \quad (5.1)$$

$$F_{\text{gas}} = \frac{1}{a_0 + a_1 T_8^{-2} + a_2 T_8^{-5}} + \frac{1.26(1 + \eta^{-1})}{1 + b_1 \eta^{-1} + b_2 \eta^{-2}}, \quad (5.2)$$

$$\eta = \frac{(\rho/\mu_e)(\text{g cm}^{-3})}{7.05 \times 10^6 T_8^{1.5} + 5.12 \times 10^4 T_8^3}, \quad (5.3)$$

$$a_0 = 23.5, \quad (5.4)$$

$$a_1 = 6.83 \times 10^4, \quad (5.5)$$

$$a_2 = 7.81 \times 10^8, \quad (5.6)$$

$$b_1 = 1.47, \quad (5.7)$$

$$b_2 = 0.0329, \quad (5.8)$$

$$G_{\text{gas}} = \frac{1}{[1 + 10^{-9}(\rho/\mu_e)](a_3 + a_4 T_8^{-2} + a_5 T_8^{-5})} + \frac{1}{b_3(\rho/\mu_e)^{-1} + b_4 + b_5(\rho/\mu_e)^{0.656}}, \quad (5.9)$$

$$a_3 = 230, \quad (5.10)$$

$$a_4 = 6.70 \times 10^5, \quad (5.11)$$

$$a_5 = 7.66 \times 10^9, \quad (5.12)$$

$$b_3 = 7.75 \times 10^5 T_8^{1.5} + 247 T_8^{3.85}, \quad (5.13)$$

$$b_4 = 4.07 + 0.0240 T_8^{1.40}, \quad (5.14)$$

$$b_5 = 4.59 \times 10^{-5} T_8^{-0.110}. \quad (5.15)$$

In the above, T_8 is the temperature in units of 10^8 K, and ρ is the mass density in units of g cm^{-3} . In passing, we note that there were typographical errors in equations (28) and (34) of Munakata et al. (1987). We have corrected these in equations (5.3) and (5.9) in the above. The present fitting formula is valid for the density-temperature region $10^0 \leq (\rho/\mu_e) \times (\text{g cm}^{-3}) \leq 10^{12}$, $10^8 \leq T(\text{K}) \leq 10^{11}$.

5.2. Liquid Metal Phase

For $T < 0.3T_F$, we use the results of the calculation of Itoh & Kohyama (1983) and Itoh et al. (1984a, b, c). In order to discuss the neutrino bremsstrahlung for strongly degenerate electrons, it is essential to specify the state of the ions. For this purpose, we introduce the parameter which measures the strength of the ionic correlation defined by

$$\Gamma \equiv \frac{Z^2 e^2}{ak_B T} = 2.275 \times 10^{-1} \frac{Z^2}{T_8} \left(\frac{\rho_6}{A} \right)^{1/3}, \quad (5.16)$$

where $a = [3/(4\pi n_i)]^{1/3}$ is the ion-sphere radius. According to Ogata & Ichimaru (1987), the ionic system is in the liquid state for $\Gamma < 180$, and it is in the crystalline lattice state for $\Gamma \geq 180$.

In the liquid metal state $\Gamma < 180$, we use the results of Itoh & Kohyama (1983). They have summarized the results of the calculation as

$$Q_{\text{liquid}} = 0.5738 (\text{ergs cm}^{-3} \text{s}^{-1}) (Z^2/A) T_8^6 \rho \times \left\{ \frac{1}{2} [(C_V^2 + C_A^2) + n(C_V'^2 + C_A'^2)] F_{\text{liquid}} - \frac{1}{2} [(C_V^2 - C_A^2) + n(C_V'^2 - C_A'^2)] G_{\text{liquid}} \right\}. \quad (5.17)$$

For the convenience of applications, they have fitted the numerical results of the calculation by analytic formulae. We introduce the following variable:

$$u = 2\pi(\log_{10} \rho - 3)/10. \quad (5.18)$$

The fitting has been carried out for the ranges $10^4 \leq \rho (\text{g cm}^{-3}) \leq 4.3 \times 10^{11}$, $1 \leq \Gamma \leq 160$. For the parameter Γ , modest extrapolations outside the above range are permissible, but not for the density parameter. The fitting formulae are taken as

$$F_{\text{liquid}}(u, \Gamma) = vF(u, 1) + (1-v)F(u, 160), \quad (5.19)$$

$$G_{\text{liquid}}(u, \Gamma) = wG(u, 1) + (1-w)G(u, 160), \quad (5.20)$$

$$F(u, 1) = \frac{a_0}{2} + \sum_{m=1}^5 a_m \cos mu + \sum_{m=1}^4 b_m \sin mu + cu + d, \quad (5.21)$$

$$F(u, 160) = \frac{e_0}{2} + \sum_{m=1}^5 e_m \cos mu + \sum_{m=1}^4 f_m \sin mu + gu + h, \quad (5.22)$$

$$G(u, 1) = \frac{i_0}{2} + \sum_{m=1}^5 i_m \cos mu + \sum_{m=1}^4 j_m \sin mu + ku + l, \quad (5.23)$$

$$G(u, 160) = \frac{p_0}{2} + \sum_{m=1}^5 p_m \cos mu + \sum_{m=1}^4 q_m \sin mu + ru + s, \quad (5.24)$$

$$v = \sum_{m=0}^3 \alpha_m \Gamma^{-m/3}, \quad (5.25)$$

$$w = \sum_{m=0}^3 \beta_m \Gamma^{-m/3}. \quad (5.26)$$

The coefficients are given in Tables 3–6.

5.3. Binary Ion Mixture

In the above we have shown the results for pure chemical compositions. The extension to binary ion mixtures is carried out as follows. Let us consider binary ion mixtures of (Z_1, A_1) and (Z_2, A_2) . Let their respective mass fractions be X_1 and X_2 ($X_1 + X_2 = 1$). Equation (5.17) should be replaced by

$$Q_{\text{liquid}} = 0.5738 (\text{ergs cm}^{-3} \text{s}^{-1}) T_8^6 \rho \times \left[X_1 \frac{Z_1^2}{A_1} \left\{ \frac{1}{2} [(C_V^2 + C_A^2) + n(C_V'^2 + C_A'^2)] F_{\text{liquid}}(\Gamma_1) - \frac{1}{2} [(C_V^2 - C_A^2) + n(C_V'^2 - C_A'^2)] G_{\text{liquid}}(\Gamma_1) \right\} + X_2 \frac{Z_2^2}{A_2} \left\{ \frac{1}{2} [(C_V^2 + C_A^2) + n(C_V'^2 + C_A'^2)] F_{\text{liquid}}(\Gamma_2) - \frac{1}{2} [(C_V^2 - C_A^2) + n(C_V'^2 - C_A'^2)] G_{\text{liquid}}(\Gamma_2) \right\} \right]. \quad (5.27)$$

TABLE 3
COEFFICIENTS IN THE FITTING FORMULAE FOR $F(u, 1)$ AND $F(u, 160)$

Coefficient	${}^4\text{He}$	${}^{12}\text{C}$	${}^{16}\text{O}$	${}^{20}\text{Ne}$	${}^{24}\text{Mg}$	${}^{28}\text{Si}$	${}^{32}\text{S}$	${}^{40}\text{Ca}$	${}^{56}\text{Fe}$
a_0	0.09037	0.17946	0.20933	0.23425	0.25567	0.27445	0.29120	0.32001	0.34888
a_1	-0.03009	-0.05821	-0.06740	-0.07503	-0.08158	-0.08734	-0.09250	-0.10142	-0.11076
a_2	-0.00564	-0.01089	-0.01293	-0.01472	-0.01632	-0.01777	-0.01910	-0.02145	-0.02349
a_3	-0.00544	-0.01147	-0.01352	-0.01522	-0.01667	-0.01793	-0.01905	-0.02094	-0.02283
a_4	-0.00290	-0.00656	-0.00776	-0.00872	-0.00952	-0.01019	-0.01076	-0.01168	-0.01250
a_5	-0.00224	-0.00519	-0.00613	-0.00688	-0.00748	-0.00798	-0.00839	-0.00902	-0.00971
b_1	-0.02148	-0.04969	-0.05950	-0.06776	-0.07491	-0.08120	-0.08682	-0.09651	-0.10661
b_2	-0.00817	-0.01584	-0.01837	-0.02045	-0.02220	-0.02370	-0.02500	-0.02716	-0.02860
b_3	-0.00300	-0.00504	-0.00567	-0.00616	-0.00653	-0.00683	-0.00706	-0.00738	-0.00785
b_4	-0.00170	-0.00281	-0.00310	-0.00331	-0.00345	-0.00356	-0.00363	-0.00370	-0.00385
c	0.00671	0.00945	0.00952	0.00932	0.00899	0.00858	0.00814	0.00721	0.00766
d	0.28130	0.34529	0.36029	0.37137	0.38006	0.38714	0.39309	0.40262	0.40991
e_0	-0.02006	0.06781	0.09304	0.11465	0.13455	0.15315	0.17049	0.20051	0.23159
e_1	0.01790	-0.00944	-0.01656	-0.02253	-0.02828	-0.03391	-0.03930	-0.04877	-0.05891
e_2	-0.00783	-0.01289	-0.01489	-0.01680	-0.01846	-0.01988	-0.02113	-0.02331	-0.02531
e_3	-0.00021	-0.00589	-0.00778	-0.00942	-0.01087	-0.01218	-0.01338	-0.01541	-0.01747
e_4	0.00024	-0.00404	-0.00520	-0.00613	-0.00693	-0.00763	-0.00825	-0.00925	-0.01021
e_5	-0.00014	-0.00330	-0.00418	-0.00488	-0.00547	-0.00596	-0.00639	-0.00705	-0.00778
f_1	0.00538	-0.02213	-0.03076	-0.03824	-0.04508	-0.05142	-0.05729	-0.06744	-0.07767
f_2	-0.00175	-0.01136	-0.01390	-0.01601	-0.01782	-0.01941	-0.02082	-0.02311	-0.02516
f_3	-0.00346	-0.00467	-0.00522	-0.00571	-0.00607	-0.00631	-0.00648	-0.00670	-0.00711
f_4	-0.00031	-0.00131	-0.00161	-0.00183	-0.00200	-0.00212	-0.00221	-0.00233	-0.00260
g	-0.02199	-0.02342	-0.02513	-0.02697	-0.02832	-0.02919	-0.02978	-0.03070	-0.03076
h	0.17300	0.24819	0.27480	0.29806	0.31541	0.32790	0.33756	0.35242	0.36908

The respective Γ values should be calculated by

$$\Gamma_i = 2.275 \times 10^{-1} \frac{Z_i^2}{T_\epsilon} \left(\frac{\rho_6 X_i}{A_i} \right)^{1/3} \quad (i = 1, 2). \quad (5.28)$$

The extension to three and higher component systems is straightforward.

5.4. Low-Temperature Quantum Corrections in the Liquid Metal Phase

The low-temperature quantum corrections in the liquid metal phase have been calculated by Itoh et al. (1984a). However, the corrections are generally small when the perturbative method is valid; they become large when the method loses its validity. Therefore, if one wishes to consider the overall behav-

TABLE 4
COEFFICIENTS IN THE FITTING FORMULAE FOR $G(u, 1)$ AND $G(u, 160)$

Coefficient	${}^4\text{He}$	${}^{12}\text{C}$	${}^{16}\text{O}$	${}^{20}\text{Ne}$	${}^{24}\text{Mg}$	${}^{28}\text{Si}$	${}^{32}\text{S}$	${}^{40}\text{Ca}$	${}^{56}\text{Fe}$
i_0	0.00192	0.00766	0.00951	0.01103	0.01231	0.01342	0.01440	0.01606	0.01892
i_1	-0.00301	-0.00710	-0.00838	-0.00942	-0.01030	-0.01106	-0.01172	-0.01285	-0.01493
i_2	-0.00073	-0.00028	-0.00011	0.00004	0.00016	0.00027	0.00037	0.00055	0.00125
i_3	0.00182	0.00232	0.00244	0.00252	0.00259	0.00264	0.00269	0.00276	0.00262
i_4	0.00037	0.00044	0.00046	0.00047	0.00048	0.00049	0.00050	0.00051	0.00055
i_5	0.00116	0.00158	0.00168	0.00176	0.00183	0.00188	0.00193	0.00201	0.00209
j_1	0.01706	0.02300	0.02455	0.02573	0.02669	0.02748	0.02816	0.02927	0.03034
j_2	-0.00753	-0.01078	-0.01167	-0.01236	-0.01291	-0.01338	-0.01379	-0.01445	-0.01519
j_3	0.00066	0.00118	0.00132	0.00144	0.00154	0.00162	0.00169	0.00181	0.00204
j_4	-0.00060	-0.00089	-0.00097	-0.00103	-0.00108	-0.00112	-0.00116	-0.00122	-0.00135
k	-0.01021	-0.01259	-0.01314	-0.01354	-0.01386	-0.01411	-0.01432	-0.01465	-0.01494
l	0.06417	0.07917	0.08263	0.08515	0.08711	0.08869	0.09001	0.09209	0.09395
p_0	-0.01112	-0.00769	-0.00700	-0.00649	-0.00583	-0.00502	-0.00415	-0.00255	-0.00011
p_1	0.00603	0.00356	0.00295	0.00246	0.00192	0.00132	0.00070	-0.00042	-0.00222
p_2	-0.00149	-0.00184	-0.00184	-0.00183	-0.00179	-0.00173	-0.00166	-0.00151	-0.00104
p_3	0.00047	0.00146	0.00166	0.00181	0.00193	0.00203	0.00211	0.00224	0.00225
p_4	0.00040	0.00031	0.00032	0.00033	0.00034	0.00034	0.00034	0.00034	0.00037
p_5	0.00028	0.00069	0.00082	0.00093	0.00102	0.00110	0.00116	0.00126	0.00140
q_1	0.00422	0.01052	0.01231	0.01379	0.01501	0.01604	0.01693	0.01841	0.02013
q_2	-0.00009	-0.00354	-0.00445	-0.00518	-0.00582	-0.00639	-0.00691	-0.00778	-0.00883
q_3	-0.00066	-0.00014	0.00002	0.00013	0.00024	0.00035	0.00045	0.00062	0.00090
q_4	-0.00003	-0.00018	-0.00026	-0.00033	-0.00038	-0.00044	-0.00048	-0.00056	-0.00071
r	-0.00561	-0.00829	-0.00921	-0.01000	-0.01059	-0.01103	-0.01136	-0.01188	-0.01249
s	0.03522	0.05211	0.05786	0.06284	0.06657	0.06928	0.07140	0.07468	0.07850

TABLE 5
 $F(u, 1)$, $F(u, 160)$, $G(u, 1)$, AND $G(u, 160)$ FOR THE
 NEUTRON STAR MATTER

ρ	Z	A	$F(u, 1)$	$F(u, 160)$	$G(u, 1)$	$G(u, 160)$
1.044E+4 ...	26	56	0.4160	0.3503	0.0848	0.0708
2.622E+4 ...	26	56	0.4418	0.3609	0.0897	0.0729
6.587E+4 ...	26	56	0.4671	0.3698	0.0953	0.0750
1.654E+5 ...	26	56	0.4928	0.3780	0.1017	0.0772
4.156E+5 ...	26	56	0.5207	0.3862	0.1087	0.0794
1.044E+6 ...	26	56	0.5525	0.3953	0.1157	0.0808
2.622E+6 ...	26	56	0.5887	0.4052	0.1201	0.0801
6.588E+6 ...	26	56	0.6268	0.4153	0.1184	0.0751
8.293E+6 ...	28	62	0.6423	0.4280	0.1183	0.0754
1.655E+7 ...	28	62	0.6693	0.4350	0.1098	0.0674
3.302E+7 ...	28	62	0.6924	0.4404	0.0968	0.0572
6.589E+7 ...	28	62	0.7108	0.4441	0.0811	0.0461
1.315E+8 ...	28	62	0.7244	0.4463	0.0648	0.0354
2.624E+8 ...	28	62	0.7340	0.4475	0.0496	0.0261
3.304E+8 ...	28	64	0.7361	0.4477	0.0456	0.0237
5.237E+8 ...	28	64	0.7401	0.4479	0.0371	0.0188
8.301E+8 ...	28	64	0.7430	0.4480	0.0298	0.0148
1.045E+9 ...	28	64	0.7442	0.4479	0.0266	0.0130
1.316E+9 ...	34	84	0.7702	0.4815	0.0256	0.0131
1.657E+9 ...	34	84	0.7710	0.4814	0.0228	0.0116
2.626E+9 ...	34	84	0.7722	0.4812	0.0178	0.0089
4.164E+9 ...	34	84	0.7729	0.4807	0.0138	0.0067
6.601E+9 ...	34	84	0.7729	0.4800	0.0107	0.0051
8.312E+9 ...	32	82	0.7649	0.4682	0.0094	0.0044
1.046E+10 ...	32	82	0.7646	0.4677	0.0082	0.0038
1.318E+10 ...	32	82	0.7642	0.4671	0.0072	0.0033
1.659E+10 ...	32	82	0.7637	0.4664	0.0063	0.0028
2.090E+10 ...	32	82	0.7630	0.4656	0.0054	0.0025
2.631E+10 ...	30	80	0.7538	0.4544	0.0048	0.0021
3.313E+10 ...	30	80	0.7529	0.4534	0.0041	0.0018
4.172E+10 ...	30	80	0.7517	0.4522	0.0036	0.0016
5.254E+10 ...	28	78	0.7415	0.4392	0.0032	0.0013
6.617E+10 ...	28	78	0.7400	0.4377	0.0027	0.0011
8.332E+10 ...	28	78	0.7382	0.4359	0.0024	0.0010
1.049E+11 ...	28	78	0.7361	0.4339	0.0020	0.0008
1.322E+11 ...	28	78	0.7336	0.4315	0.0018	0.0007
1.664E+11 ...	26	76	0.7218	0.4164	0.0015	0.0006
1.844E+11 ...	42	124	0.7758	0.4917	0.0016	0.0007
2.096E+11 ...	40	122	0.7681	0.4813	0.0015	0.0007
2.640E+11 ...	40	122	0.7632	0.4766	0.0013	0.0006
3.325E+11 ...	38	120	0.7524	0.4624	0.0011	0.0005
4.188E+11 ...	36	118	0.7346	0.4436	0.0010	0.0004
4.299E+11 ...	36	118	0.7338	0.4428	0.0010	0.0004
4.635E+11 ...	40	180	0.7515	0.4653	0.0012	0.0005
6.645E+11 ...	40	200	0.7434	0.4574	0.0010	0.0004
9.967E+11 ...	40	250	0.7368	0.4511	0.0009	0.0004
1.460E+12 ...	40	320	0.7315	0.4460	0.0008	0.0003
2.641E+12 ...	40	500	0.7252	0.4400	0.0007	0.0003
6.196E+12 ...	50	950	0.7181	0.4448	0.0006	0.0002
9.585E+12 ...	50	1100	0.6988	0.4262	0.0005	0.0002
1.480E+13 ...	50	1350	0.6816	0.4097	0.0004	0.0002
3.389E+13 ...	50	1800	0.6346	0.3647	0.0003	0.0001
7.890E+13 ...	40	1500	0.5485	0.2731	0.0001	0.0000
1.311E+14 ...	32	982	0.4677	0.1914	0.0001	0.0000

TABLE 6
 COEFFICIENTS IN THE FITTING FORMULAE FOR v AND w

Coefficient	${}^4\text{He}$	${}^{12}\text{C}$	${}^{16}\text{O}$	${}^{20}\text{Ne}$	${}^{24}\text{Mg}$	${}^{28}\text{Si}$	${}^{32}\text{S}$	${}^{40}\text{Ca}$	${}^{56}\text{Fe}$	Neutron Star Matter
α_0	-0.07980	-0.05483	-0.06597	-0.06910	-0.07003	-0.07023	-0.06814	-0.06934	-0.07608	-0.07913
α_1	0.17057	-0.01946	0.06048	0.07685	0.07808	0.07660	0.05799	0.06443	0.11559	0.13177
α_2	1.51980	1.86310	1.74860	1.74280	1.75870	1.77560	1.81880	1.82500	1.75730	1.74940
α_3	-0.61058	-0.78873	-0.74308	-0.75047	-0.76675	-0.78191	-0.80866	-0.82010	-0.79677	-0.80199
β_0	-0.05881	-0.06711	-0.07356	-0.07123	-0.06960	-0.06983	-0.06880	-0.07255	-0.08034	-0.06778
β_1	0.00165	0.06859	0.10865	0.08264	0.06577	0.06649	0.05775	0.08529	0.14368	0.06268
β_2	1.82700	1.74360	1.70150	1.76760	1.81180	1.82170	1.84540	1.81230	1.73140	1.78740
β_3	-0.76993	-0.74498	-0.73653	-0.77896	-0.80797	-0.81839	-0.83439	-0.82499	-0.79467	-0.78226

ior of the neutrino bremsstrahlung, it would not be too unreasonable to neglect the low-temperature quantum corrections altogether. We recommend this treatment to the reader who wishes to incorporate the present result into his/her computer code of stellar evolution.

5.5. Crystalline Lattice Phase

The energy-loss rates caused by the neutrino bremsstrahlung in the crystalline lattice phase have been calculated by Itoh et al. (1984b, c). The former paper gives a comprehensive description of the analytical fitting formulae. There are two kinds of contributions to the neutrino bremsstrahlung in the crystalline lattice phase: one is the static lattice contribution and the other is the phonon contribution. In order to obtain the total neutrino energy-loss rate in the lattice phase, one takes $Q_{\text{lattice}} + Q_{\text{phonon}}$. The fitting has been carried out for the range $10^4 \leq \rho (\text{g cm}^{-3}) \leq 10^{12}$, $171 \leq \Gamma \leq 5000$. The results of F_{lattice} and G_{lattice} for $\Gamma > 5000$ are almost identical to the results for $\Gamma = 5000$. The results of F_{phonon} and G_{phonon} for $\Gamma > 5000$ can be obtained by extrapolating the formulae for $\Gamma \leq 5000$. The analytical fitting formulae are as follows:

$$Q_{\text{crystal}} = Q_{\text{lattice}} + Q_{\text{phonon}}, \quad (5.29)$$

$$u = 2\pi(\log_{10} \rho - 3)/9, \quad (5.30)$$

$$Q_{\text{lattice}} = 0.5738 [\text{ergs cm}^{-3} \text{s}^{-1}] (Z^2/A) T_8^6 \rho f_{\text{band}} \times \left\{ \frac{1}{2}[(C_V^2 + C_A^2) + n(C_V'^2 + C_A'^2)] F_{\text{lattice}} - \frac{1}{2}[(C_V^2 - C_A^2) + n(C_V'^2 - C_A'^2)] G_{\text{lattice}} \right\}, \quad (5.31)$$

$$f_{\text{band}} = \exp(-2V_{\text{band}}/k_B T), \quad (5.32)$$

$$2V_{\text{band}}/k_B T = 0.00119 Z^{2/3} \hbar k_F c / k_B T = 7.12 \times 10^{-2} Z(\rho_6/A)^{1/3} T_8^{-1}, \quad (5.33)$$

$$Q_{\text{phonon}} = 0.5738 [\text{ergs cm}^{-3} \text{s}^{-1}] (Z^2/A) T_8^6 \rho \times \left\{ \frac{1}{2}[(C_V^2 + C_A^2) + n(C_V'^2 + C_A'^2)] F_{\text{phonon}} - \frac{1}{2}[(C_V^2 - C_A^2) + n(C_V'^2 - C_A'^2)] G_{\text{phonon}} \right\}, \quad (5.34)$$

$$F_{\text{lattice}}(u, \Gamma) = (1 - v)F(u, 171) + vF(u, 5000), \quad (5.35)$$

$$G_{\text{lattice}}(u, \Gamma) = (1 - w)G(u, 171) + wG(u, 5000), \quad (5.36)$$

$$F_{\text{phonon}} = v'F'(u, 171), \quad (5.37)$$

$$G_{\text{phonon}} = w'G'(u, 171), \quad (5.38)$$

$$F(u, 171) = \frac{a_0}{2} + \sum_{m=1}^4 a_m \cos mu + \sum_{m=1}^3 b_m \sin mu + cu + d, \quad (5.39)$$

$$F(u, 5000) = \frac{e_0}{2} + \sum_{m=1}^4 e_m \cos mu + \sum_{m=1}^3 f_m \sin mu + gu + h, \quad (5.40)$$

$$G(u, 171) = \frac{i_0}{2} + \sum_{m=1}^4 i_m \cos mu + \sum_{m=1}^3 j_m \sin mu + ku + l, \quad (5.41)$$

$$G(u, 5000) = \frac{p_0}{2} + \sum_{m=1}^4 p_m \cos mu + \sum_{m=1}^3 q_m \sin mu + ru + s, \quad (5.42)$$

$$F'(u, 171) = \frac{a'_0}{2} + \sum_{m=1}^4 a'_m \cos mu + \sum_{m=1}^3 b'_m \sin mu + c'u + d', \quad (5.43)$$

$$G'(u, 171) = \frac{i'_0}{2} + \sum_{m=1}^4 i'_m \cos mu + \sum_{m=1}^3 j'_m \sin mu + k'u + l', \quad (5.44)$$

$$v = \sum_{m=0}^3 \alpha_m \Gamma^{-m/3}, \quad (5.45)$$

$$w = \sum_{m=0}^3 \beta_m \Gamma^{-m/3}, \quad (5.46)$$

$$v' = \sum_{m=0}^3 \alpha'_m \Gamma^{-m/3}, \quad (5.47)$$

$$w' = \sum_{m=0}^3 \beta'_m \Gamma^{-m/3}. \quad (5.48)$$

The coefficients are given in Tables 7–11. In equations (5.31) and (5.32), f_{band} is the factor which semiquantitatively takes into account the reduction of Q_{lattice} resulting from the existence of the band gap in the electronic states (Pethick & Thorsson 1994). The band gap $2V_{\text{band}}$ is calculated using the smallest reciprocal lattice vector of the original body-centered cubic lattice. Equation (5.32) is not an exact functional form, but it expresses the most important effect caused by the existence of the band gap in the electronic states.

One should note that there generally exist two kinds of discontinuities in the bremsstrahlung neutrino energy-loss rates. The first discontinuity corresponds to the boundary between the weakly degenerate electron phase and the liquid metal phase. In principle, there should be no discontinuous change across this boundary. In practice, however, the present status of the theoretical calculations brings about an undesired discontinuity, since the general calculation which is valid for the two phases is too involved at the present stage. The amount of the discontinuity across the boundary shows a measure of the theoretical uncertainty for this intermediate region.

The second discontinuity corresponds to the liquid-solid phase transition of the ionic system. The discontinuity in the neutrino energy-loss rates across this transition point is a genuine physical discontinuity. This is analogous to the disconti-

TABLE 7
COEFFICIENTS IN THE FITTING FORMULAE FOR $F(u, 171)$ AND $F(u, 5000)$

Coefficient	${}^4\text{He}$	${}^{12}\text{C}$	${}^{16}\text{O}$	${}^{20}\text{Ne}$	${}^{24}\text{Mg}$	${}^{28}\text{Si}$	${}^{32}\text{S}$	${}^{40}\text{Ca}$	${}^{56}\text{Fe}$
a_0	-0.02296	0.03677	0.03232	0.03224	0.03191	0.03318	0.03471	0.03754	0.04192
a_1	0.01601	-0.01066	-0.00874	-0.01010	-0.01083	-0.01218	-0.01341	-0.01521	-0.01768
a_2	-0.00433	-0.00458	-0.00413	-0.00285	-0.00211	-0.00145	-0.00098	-0.00052	-0.00007
a_3	0.00015	-0.00177	-0.00190	-0.00193	-0.00192	-0.00197	-0.00204	-0.00218	-0.00241
a_4	-0.00034	-0.00138	-0.00139	-0.00123	-0.00109	-0.00099	-0.00093	-0.00086	-0.00080
b_1	0.01558	-0.00244	-0.00344	-0.00607	-0.00753	-0.00940	-0.01107	-0.01349	-0.01705
b_2	0.00191	-0.00206	-0.00261	-0.00279	-0.00281	-0.00281	-0.00280	-0.00280	-0.00268
b_3	-0.00055	-0.00037	-0.00070	-0.00078	-0.00087	-0.00093	-0.00100	-0.00115	-0.00141
c	-0.01694	-0.01093	-0.00791	-0.00365	-0.00110	0.00123	0.00304	0.00531	0.00818
d	0.10649	0.12431	0.13980	0.13861	0.14075	0.13959	0.13847	0.13927	0.13629
e_0	-0.03654	0.04719	0.04421	0.05766	0.06145	0.06964	0.07593	0.08106	0.09256
e_1	0.02395	-0.01353	-0.00883	-0.01613	-0.01751	-0.02211	-0.02568	-0.02720	-0.03290
e_2	-0.00448	-0.00619	-0.00857	-0.00739	-0.00750	-0.00656	-0.00575	-0.00613	-0.00523
e_3	-0.00033	-0.00211	-0.00257	-0.00309	-0.00340	-0.00379	-0.00413	-0.00460	-0.00539
e_4	-0.00088	-0.00176	-0.00214	-0.00222	-0.00231	-0.00236	-0.00240	-0.00260	-0.00276
f_1	0.0173	0.00456	0.00629	-0.00079	-0.00322	-0.00863	-0.01332	-0.01665	-0.02574
f_2	0.00402	-0.00174	-0.00210	-0.00328	-0.00386	-0.00450	-0.00495	-0.00559	-0.00630
f_3	-0.00005	-0.00031	-0.00099	-0.00115	-0.00148	-0.00162	-0.00177	-0.00229	-0.00285
g	-0.02222	-0.02259	-0.02610	-0.01999	-0.01798	-0.01325	-0.00913	-0.00698	0.00022
h	0.13969	0.20343	0.26993	0.27099	0.29179	0.29081	0.28946	0.31671	0.31871

TABLE 8
COEFFICIENTS IN THE FITTING FORMULAE FOR $G(u, 171)$ AND $G(u, 5000)$

Coefficient	${}^4\text{He}$	${}^{12}\text{C}$	${}^{16}\text{O}$	${}^{20}\text{Ne}$	${}^{24}\text{Mg}$	${}^{28}\text{Si}$	${}^{32}\text{S}$	${}^{40}\text{Ca}$	${}^{56}\text{Fe}$
i_0	-0.00647	0.00106	0.00199	0.00362	0.00468	0.00573	0.00662	0.00789	0.00977
i_1	0.00440	-0.00048	-0.00112	-0.00224	-0.00297	-0.00370	-0.00432	-0.00520	-0.00653
i_2	-0.00110	-0.00022	-0.00003	0.00031	0.00053	0.00076	0.00096	0.00123	0.00171
i_3	0.00001	0.00019	0.00014	0.00009	0.00004	0.00000	-0.00004	-0.00010	-0.00024
i_4	-0.00007	-0.00001	0.00001	0.00003	0.00005	0.00007	0.00009	0.00012	0.00017
j_1	0.00294	0.00658	0.00745	0.00778	0.00810	0.00826	0.00839	0.00865	0.00869
j_2	0.00059	-0.00180	-0.00209	-0.00241	-0.00261	-0.00279	-0.00293	-0.00312	-0.00323
j_3	-0.00018	0.00036	0.00044	0.00054	0.00059	0.00065	0.00068	0.00073	0.00075
k	-0.00337	-0.00398	-0.00447	-0.00444	-0.00451	-0.00448	-0.00445	-0.00448	-0.00439
l	0.02116	0.02499	0.02811	0.02793	0.02840	0.02820	0.02800	0.02820	0.02766
p_0	-0.00938	-0.00047	-0.00111	0.00240	0.00384	0.00636	0.00848	0.01025	0.01464
p_1	0.00610	0.00063	0.00110	-0.00124	-0.00219	-0.00389	-0.00534	-0.00652	-0.00957
p_2	-0.00114	-0.00064	-0.00074	-0.00019	0.00005	0.00050	0.00091	0.00123	0.00222
p_3	-0.00010	0.00030	0.00024	0.00022	0.00017	0.00013	0.00008	0.00001	-0.00022
p_4	-0.00018	-0.00006	-0.00004	0.00001	0.00004	0.00008	0.00011	0.00016	0.00025
q_1	0.00320	0.01013	0.01286	0.01396	0.01526	0.01587	0.01632	0.01790	0.01867
q_2	0.00107	-0.00247	-0.00281	-0.00366	-0.00412	-0.00465	-0.00506	-0.00556	-0.00615
q_3	-0.00008	0.00052	0.00057	0.00077	0.00086	0.00100	0.00111	0.00119	0.00133
r	-0.00442	-0.00650	-0.00861	-0.00866	-0.00933	-0.00931	-0.00928	-0.01015	-0.01023
s	0.02775	0.04087	0.05414	0.05448	0.05868	0.05857	0.05837	0.06388	0.06442

TABLE 9
COEFFICIENTS IN THE FITTING FORMULAE FOR $F'(u, 171)$ AND $G'(u, 171)$

Coefficient	${}^4\text{He}$	${}^{12}\text{C}$	${}^{16}\text{O}$	${}^{20}\text{Ne}$	${}^{24}\text{Mg}$	${}^{28}\text{Si}$	${}^{32}\text{S}$	${}^{40}\text{Ca}$	${}^{56}\text{Fe}$
a'_0	-0.01373	0.02231	0.01599	0.01672	0.01608	0.01767	0.01927	0.02137	0.02584
a'_1	0.00957	-0.00589	-0.00191	-0.00325	-0.00329	-0.00455	-0.00567	-0.00661	-0.00894
a'_2	-0.00204	-0.00279	-0.00330	-0.00248	-0.00222	-0.00177	-0.00143	-0.00134	-0.00097
a'_3	-0.00005	-0.00073	-0.00075	-0.00078	-0.00078	-0.00084	-0.00091	-0.00103	-0.00125
a'_4	-0.00003	-0.00043	-0.00047	-0.00045	-0.00042	-0.00041	-0.00041	-0.00043	-0.00045
b'_1	0.00661	-0.00095	0.00088	-0.00080	-0.00108	-0.00244	-0.00365	-0.00477	-0.00739
b'_2	0.00135	-0.00059	-0.00098	-0.00128	-0.00138	-0.00152	-0.00162	-0.00175	-0.00190
b'_3	-0.00035	0.00002	-0.00036	-0.00037	-0.00044	-0.00044	-0.00045	-0.00054	-0.00062
c'	-0.00811	-0.00729	-0.00776	-0.00500	-0.00399	-0.00239	-0.00113	-0.00029	0.00167
d'	0.05098	0.06630	0.08995	0.08939	0.09525	0.09466	0.09407	0.10004	0.09950
i'_0	-0.00338	0.00024	-0.00017	0.00092	0.00137	0.00213	0.00277	0.00343	0.00480
i'_1	0.00231	0.00018	0.00055	-0.00017	-0.00044	-0.00094	-0.00137	-0.00178	-0.00271
i'_2	-0.00047	-0.00028	-0.00038	-0.00022	-0.00015	-0.00003	0.00008	0.00018	0.00047
i'_3	-0.00003	0.00012	0.00011	0.00011	0.00011	0.00010	0.00009	0.00007	0.00001
i'_4	0.00000	-0.00004	-0.00003	-0.00003	-0.00003	-0.00003	-0.00003	-0.00003	-0.00001
j'_1	0.00111	0.00339	0.00429	0.00461	0.00500	0.00520	0.00535	0.00579	0.00604
j'_2	0.00042	-0.00082	-0.00088	-0.00115	-0.00129	-0.00146	-0.00159	-0.00176	-0.00197
j'_3	-0.00010	0.00015	0.00014	0.00022	0.00025	0.00030	0.00034	0.00038	0.00044
k'	-0.00161	-0.00212	-0.00287	-0.00286	-0.00304	-0.00303	-0.00301	-0.00321	-0.00320
l'	0.01013	0.01332	0.01803	0.01796	0.01915	0.01906	0.01896	0.02018	0.02012

TABLE 10
 $F(u, 171)$, $F(u, 5000)$, $G(u, 171)$, $G(u, 5000)$, $F'(u, 171)$, AND $G'(u, 171)$ FOR THE NEUTRON STAR MATTER

ρ	Z	A	$F(u, 171)$	$F(u, 5000)$	$G(u, 171)$	$G(u, 5000)$	$F'(u, 171)$	$G'(u, 171)$
1.044E+4 ...	26	56	0.1366	0.3192	0.0277	0.0645	0.0997	0.0201
2.622E+4 ...	26	56	0.1423	0.3289	0.0289	0.0665	0.1027	0.0208
6.587E+4 ...	26	56	0.1477	0.3372	0.0303	0.0685	0.1055	0.0214
1.654E+5 ...	26	56	0.1534	0.3451	0.0318	0.0707	0.1081	0.0222
4.156E+5 ...	26	56	0.1602	0.3535	0.0337	0.0730	0.1110	0.0229
1.044E+6 ...	26	56	0.1686	0.3631	0.0355	0.0747	0.1143	0.0235
2.622E+6 ...	26	56	0.1785	0.3738	0.0365	0.0742	0.1180	0.0235
6.588E+6 ...	26	56	0.1888	0.3844	0.0354	0.0698	0.1217	0.0221
8.293E+6 ...	28	62	0.1935	0.4057	0.0353	0.0710	0.1261	0.0222
1.655E+7 ...	28	62	0.2004	0.4100	0.0322	0.0631	0.1283	0.0199
3.302E+7 ...	28	62	0.2059	0.4131	0.0277	0.0533	0.1299	0.0168
6.589E+7 ...	28	62	0.2099	0.4148	0.0226	0.0428	0.1311	0.0135
1.315E+8 ...	28	62	0.2125	0.4153	0.0175	0.0327	0.1317	0.0103
2.624E+8 ...	28	62	0.2141	0.4149	0.0129	0.0239	0.1320	0.0076
3.304E+8 ...	28	64	0.2144	0.4148	0.0118	0.0217	0.1321	0.0069
5.237E+8 ...	28	64	0.2150	0.4141	0.0094	0.0172	0.1321	0.0055
8.301E+8 ...	28	64	0.2153	0.4131	0.0073	0.0134	0.1321	0.0043
1.045E+9 ...	28	64	0.2154	0.4126	0.0065	0.0118	0.1321	0.0038
1.316E+9 ...	34	84	0.2254	0.4476	0.0064	0.0120	0.1421	0.0038
1.657E+9 ...	34	84	0.2255	0.4472	0.0056	0.0106	0.1421	0.0033
2.626E+9 ...	34	84	0.2256	0.4462	0.0043	0.0081	0.1411	0.0025
4.164E+9 ...	34	84	0.2256	0.4449	0.0033	0.0061	0.1410	0.0019
6.601E+9 ...	34	84	0.2254	0.4434	0.0025	0.0046	0.1408	0.0015
8.312E+9 ...	32	82	0.2222	0.4318	0.0022	0.0040	0.1378	0.0013
1.046E+10 ...	32	82	0.2220	0.4308	0.0019	0.0034	0.1377	0.0011
1.318E+10 ...	32	82	0.2218	0.4297	0.0016	0.0030	0.1375	0.0009
1.659E+10 ...	32	82	0.2216	0.4284	0.0014	0.0025	0.1373	0.0008
2.090E+10 ...	32	82	0.2213	0.4271	0.0012	0.0022	0.1370	0.0007
2.631E+10 ...	30	80	0.2176	0.4140	0.0010	0.0019	0.1337	0.0006
3.313E+10 ...	30	80	0.2172	0.4123	0.0009	0.0016	0.1334	0.0005
4.172E+10 ...	30	80	0.2168	0.4105	0.0008	0.0014	0.1330	0.0004
5.254E+10 ...	28	78	0.2126	0.3959	0.0007	0.0012	0.1293	0.0004
6.617E+10 ...	28	78	0.2120	0.3937	0.0006	0.0010	0.1288	0.0003
8.332E+10 ...	28	78	0.2113	0.3912	0.0005	0.0009	0.1282	0.0003
1.049E+11 ...	28	78	0.2104	0.3885	0.0004	0.0007	0.1276	0.0002
1.322E+11 ...	28	78	0.2095	0.3854	0.0004	0.0006	0.1268	0.0002
1.644E+11 ...	26	76	0.2044	0.3697	0.0003	0.0005	0.1228	0.0002
1.844E+11 ...	42	124	0.2274	0.4524	0.0004	0.0007	0.1431	0.0002
2.096E+11 ...	40	122	0.2245	0.4419	0.0003	0.0006	0.1405	0.0002
2.640E+11 ...	40	122	0.2229	0.4370	0.0003	0.0005	0.1391	0.0002
3.325E+11 ...	38	120	0.2188	0.4236	0.0002	0.0004	0.1355	0.0001
4.188E+11 ...	36	118	0.2143	0.4093	0.0002	0.0004	0.1317	0.0001
4.299E+11 ...	36	118	0.2140	0.4086	0.0002	0.0004	0.1315	0.0001
4.634E+11 ...	40	180	0.2190	0.4281	0.0002	0.0004	0.1359	0.0001
6.644E+11 ...	40	200	0.2163	0.4203	0.0002	0.0004	0.1336	0.0001
9.966E+11 ...	40	250	0.2141	0.4140	0.0002	0.0003	0.1318	0.0001
1.460E+12 ...	40	320	0.2122	0.4090	0.0002	0.0003	0.1303	0.0001
2.641E+12 ...	40	500	0.2101	0.4031	0.0001	0.0003	0.1286	0.0001
6.196E+12 ...	50	950	0.2106	0.4109	0.0001	0.0002	0.1294	0.0001
9.585E+12 ...	50	1100	0.2041	0.3931	0.0001	0.0002	0.1241	0.0001
1.480E+13 ...	50	1350	0.1982	0.3773	0.0001	0.0001	0.1194	0.0000
3.389E+13 ...	50	1800	0.1814	0.3346	0.0001	0.0001	0.1063	0.0000
7.890E+13 ...	40	1500	0.1428	0.2446	0.0000	0.0000	0.0788	0.0000
1.311E+14 ...	32	982	0.1027	0.1644	0.0000	0.0000	0.0535	0.0000

TABLE 11
 COEFFICIENTS IN THE FITTING FORMULAE FOR v , w , v' , AND w'

Coefficient	^4He	^{12}C	^{16}O	^{20}Ne	^{24}Mg	^{28}Si	^{32}S	^{40}Ca	^{56}Fe	Neutron Star Matter
α_0	1.6449	0.6252	0.4889	0.4993	0.5104	0.5502	0.5962	0.5793	0.6798	0.6808
α_1	-23.2588	10.6819	16.1962	15.8082	16.1851	15.4934	14.4670	15.1152	12.7527	12.9514
α_2	272.1670	-70.6879	-138.4860	-134.0100	-147.1310	-148.0760	-144.0690	-151.6510	-140.1800	-145.0630
α_3	-1074.7000	-44.3349	185.7060	171.0490	230.5050	250.3260	251.8580	276.8910	268.8290	289.6790
β_0	1.6443	0.6307	0.5111	0.5366	0.5855	0.6380	0.6814	0.7331	0.7783	0.7398
β_1	-23.2414	10.4966	15.4195	15.4573	14.5626	13.3510	12.3005	11.2258	10.2315	10.9457
β_2	272.0080	-68.7973	-130.1540	-141.5810	-141.7690	-136.2650	-130.5920	-127.8900	-124.2640	-124.3540
β_3	-1074.2500	-50.0581	159.6050	217.6680	237.9640	235.7860	229.2470	238.5240	241.3060	226.3790
α'_0	-0.1394	0.5481	0.3173	0.3167	0.2524	0.2448	0.2617	0.2427	0.2847	0.2463
α'_1	7.0680	-20.4731	-14.4048	-14.2426	-12.4235	-12.1275	-12.4639	-12.2010	-13.0828	-12.1573
α'_2	-115.5940	223.9220	186.9100	183.2260	172.5400	173.0720	177.6570	180.4920	192.5030	190.2310
α'_3	619.9170	-534.9400	-476.8100	-461.2490	-446.9220	-457.7020	-475.7000	-496.3580	-543.1480	-552.5950
β'_0	-0.1394	0.5413	0.3073	0.2475	0.2521	0.2809	0.3088	0.3205	0.3221	0.3082
β'_1	7.0664	-20.2069	-13.7973	-12.0132	-12.0769	-12.7225	-13.3769	-13.7451	-13.8640	-13.2025
β'_2	-115.5800	220.7060	176.9940	165.9970	170.6080	177.8420	184.6140	194.3840	201.0700	186.3220
β'_3	619.8790	-524.1240	-438.7520	-422.3750	-446.8310	-472.0400	-494.2780	-539.2810	-573.1160	-509.1340

TABLE 12
 NUMERICAL VALUES FOR COEFFICIENTS OF THE RECOMBINATION NEUTRINO FITTING FORMULA

	a_1	a_2	a_3	b	c	d	f_1	f_2	f_3
$-20 \leq \nu < 0$	$1.51E-2$	$2.42E-1$	$1.21E+0$	$3.71E-2$	$9.06E-1$	$9.28E-1$	$0.00E+0$	$0.00E+0$	$0.00E+0$
$0 < \nu \leq 10$	$1.23E-2$	$2.66E-1$	$1.30E+0$	$1.17E-1$	$8.97E-1$	$1.77E-1$	$-1.20E-2$	$2.29E-2$	$-1.04E-3$

nity in electrical conductivity or thermal conductivity across the melting curve.

In order to clarify the existence of these different regimes of the density and temperature, we choose to express the numerical results of the bremsstrahlung neutrino loss rates by analytical fitting formulae rather than showing the numerical data in a tabular form.

6. RECOMBINATION NEUTRINO PROCESS

Kohyama et al. (1993) calculated the energy-loss rate resulting from the recombination neutrino process in the framework of the Weinberg-Salam theory. They accurately took into account the Coulomb distortion effects for the electrons in the continuum states. Their calculation supersedes those of Pinaev (1964) and Beaudet et al. (1967).

Their calculation is valid for nonrelativistic electrons. Therefore, the density and the temperature must satisfy the following conditions:

$$\rho/\mu_e \ll 10^6 \text{ g cm}^{-3}, \quad (6.1)$$

$$T \ll 6 \times 10^9 \text{ K}. \quad (6.2)$$

The more stringent condition on the density is that the K-shell state of the atom should exist. We express this condition by

$$E_F(\rho) \leq Z^2 \text{ ryd}, \quad (6.3)$$

where $E_F(\rho)$ is the electron Fermi level at zero temperature and at a given mass density ρ . Numerically, equation (6.3) can be rewritten as

$$\rho/\mu_e \leq 0.378Z^3 \text{ g cm}^{-3}. \quad (6.4)$$

Thus, we have $\rho \leq 1.63 \times 10^2 \text{ g cm}^{-3}$ for ^{12}C and $\rho \leq 1.43 \times 10^4 \text{ g cm}^{-3}$ for ^{56}Fe . Electrons are nonrelativistic at these densities.

The energy-loss rate per unit volume per unit time attributable to the recombination neutrino process is written as

$$Q_{\text{recomb}} = [(C_V^2 + \frac{3}{2}C_A^2) + n(C_V^2 + \frac{3}{2}C_A^2)] \times 2.649 \times 10^{-18} \frac{Z^{14}}{A} \rho \frac{1}{e^{\zeta+\nu} + 1} J(\text{ergs cm}^{-3} \text{ s}^{-1}), \quad (6.5)$$

$$J = \int_0^\infty dx (1+x)^3 \frac{\exp(-4x^{-1/2} \cot^{-1} x^{-1/2})}{1 - \exp(-2\pi x^{-1/2})} \frac{1}{e^{x\zeta-\nu} + 1}, \quad (6.6)$$

$$\zeta = \frac{I}{k_B T} = \frac{1.579 \times 10^5 Z^2}{T(\text{K})}, \quad (6.7)$$

$$\nu = \frac{\mu}{k_B T}, \quad (6.8)$$

where ρ is measured in units of grams per cubic centimeter, I is the ionization energy of the K-shell electron Z^2 ryd, and μ is the chemical potential of the electron. When the electrons are

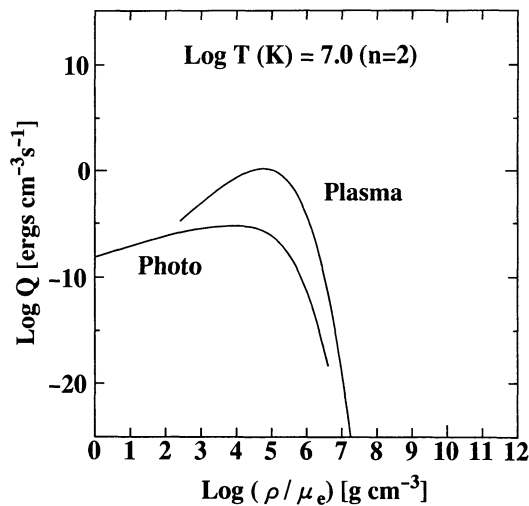


FIG. 1.—Neutrino energy-loss rates resulting from pair (below the smallest magnitude in the figure), photo-, and plasma neutrino processes for $T = 10^7$ K. The present and the following figures are drawn with the use of the exact numerical tables.

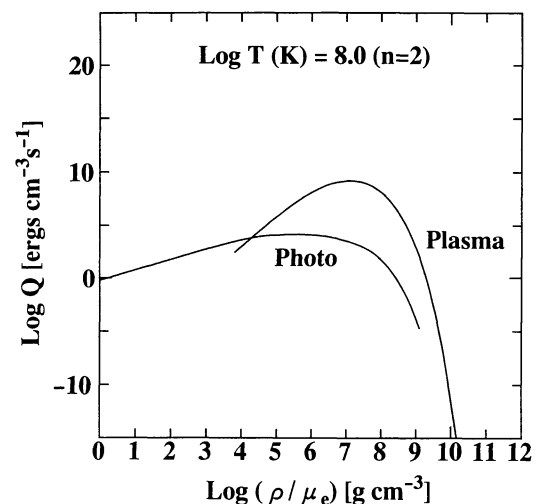
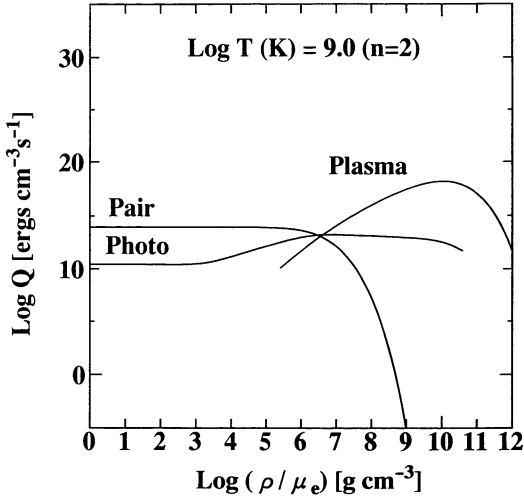
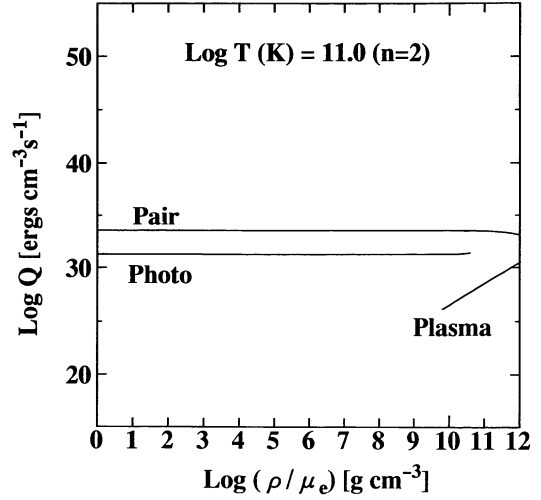


FIG. 2.—Same as Fig. 1, for $T = 10^8$ K

FIG. 3.—Same as Fig. 1, for $T = 10^9$ K.FIG. 5.—Same as Fig. 1, for $T = 10^{11}$ K.

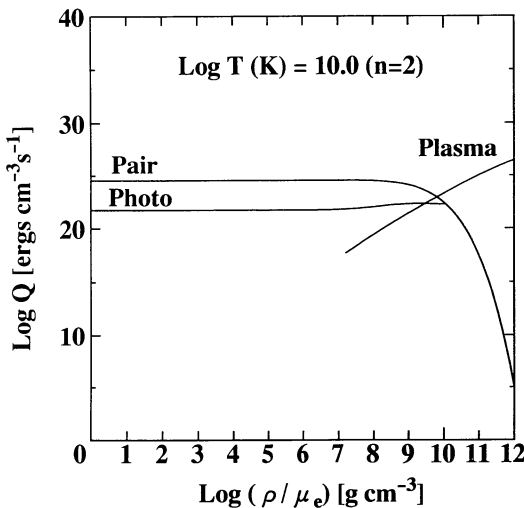
nonrelativistic, the chemical potential parameter $\nu = \mu/k_B T$ is given by (Itoh, Kojo, & Nakagawa 1990)

$$5.526 \times 10^7 \frac{\rho}{T^{3/2}} \left(1 + \frac{0.992X}{1.008} \right) = F_{1/2}(\nu), \quad (6.9)$$

$$F_{1/2}(\nu) = \int_0^\infty dx \frac{x^{1/2}}{e^{x-\nu} + 1}, \quad (6.10)$$

where X is the mass fraction of hydrogen, and the temperature is measured in kelvins. Equation (6.9) is for heavy elements with $Z/A = \frac{1}{2}$. For the heavy elements with $Z/A \neq \frac{1}{2}$, the following formula should replace equation (6.9):

$$5.526 \times 10^7 \frac{\rho}{T^{3/2}} \frac{2Z}{A} = F_{1/2}(\nu). \quad (6.11)$$

FIG. 4.—Same as Fig. 1, for $T = 10^{10}$ K.

In order to facilitate applications, we give an analytic fitting formula for the factor J in equation (6.5):

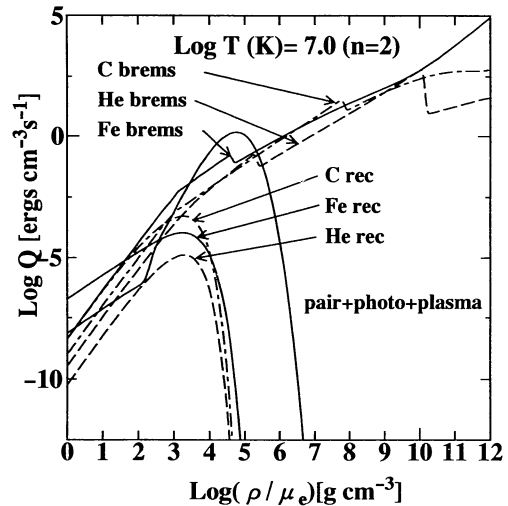
$$J = \frac{(a_1 z^{-1} + a_2 z^{-2.25} + a_3 z^{-4.55}) e^\nu}{1 + b e^{\alpha\nu} (1 + dz)}, \quad (6.12)$$

$$z = \frac{\xi}{1 + f_1 \nu + f_2 \nu^2 + f_3 \nu^3}, \quad (6.13)$$

where the coefficients are given in Table 12. The accuracy of the fitting formula is better than 11% in the density-temperature region considered in this section, $1 \leq Z \leq 26$, $10^{-3} \leq \xi \leq 10^1$, $-20 \leq \nu \leq 10$.

7. COMPARISON OF VARIOUS NEUTRINO PROCESSES

In Figures 1–10 we show the contributions of the various neutrino processes for the case of $\sin^2 \theta_w = 0.2319$ and $n = 2$,

FIG. 6.—Neutrino energy-loss rates resulting from bremsstrahlung and recombination processes for $T = 10^7$ K.

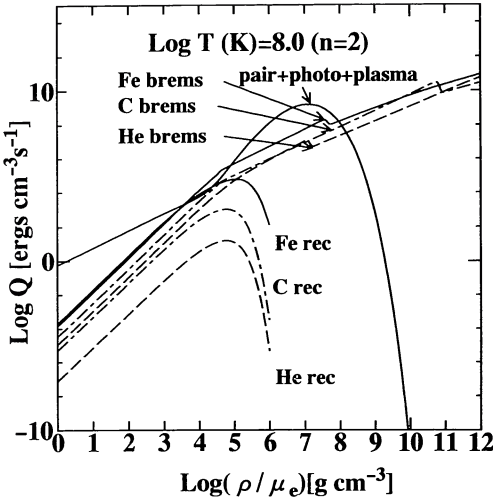


FIG. 7.—Same as Fig. 6, for $T = 10^8$ K

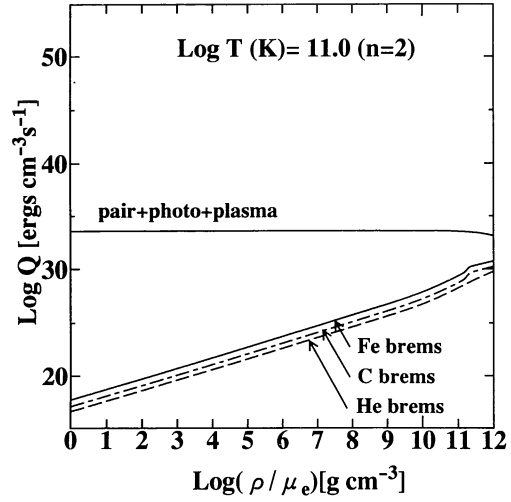


FIG. 10.—Same as Fig. 6, for $T = 10^{11}$ K

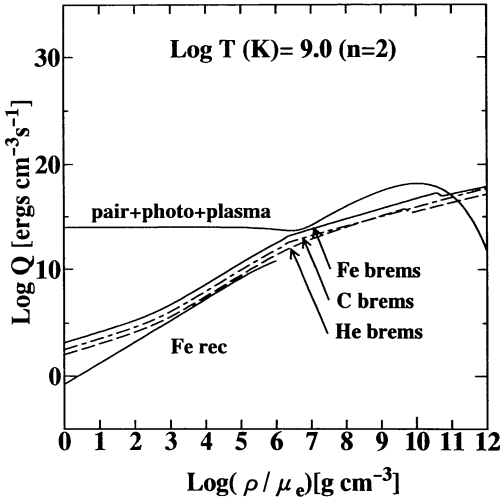


FIG. 8.—Same as Fig. 6, for $T = 10^9$ K

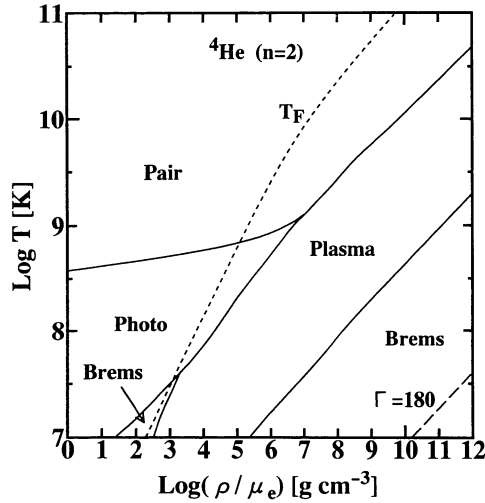


FIG. 11.—Most dominant neutrino process for a given density and temperature in the case of ${}^4\text{He}$ matter. T_F is the electron Fermi temperature given by eq. (4.3). The line marked " $\Gamma = 180$ " is the melting curve of the ionic Coulomb solid.

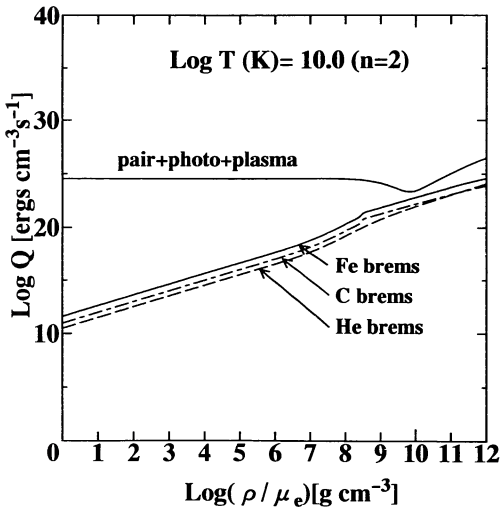


FIG. 9.—Same as Fig. 6, for $T = 10^{10}$ K

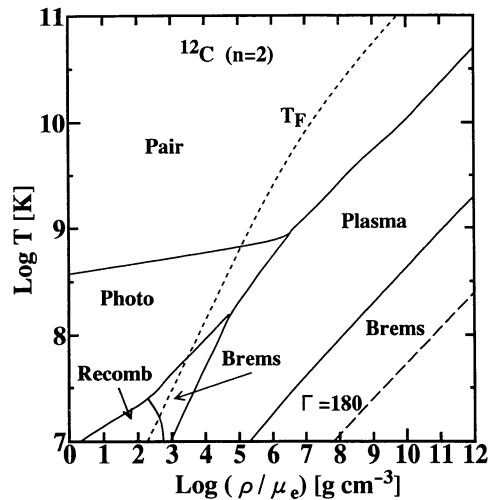


FIG. 12.—Same as Fig. 11, in the case of ${}^{12}\text{C}$ matter

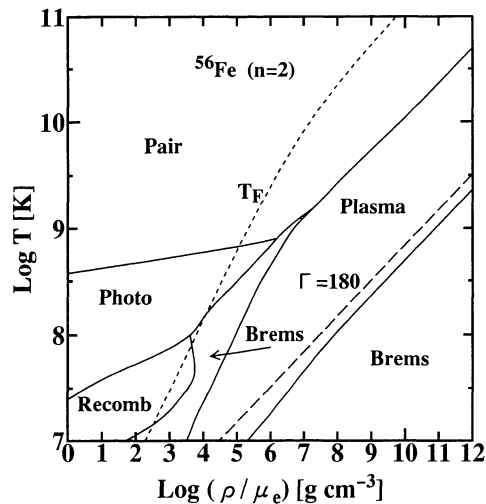


FIG. 13.—Same as Fig. 13, in the case of ^{56}Fe matter

considering the three chemical elements of ^4He , ^{12}C , and ^{56}Fe , corresponding to the temperatures $T = 10^7$, 10^8 , 10^9 , 10^{10} , and 10^{11} K. In Figures 11–13 we show the most dominant neu-

trino process for a given density and temperature for the three chemical elements of ^4He , ^{12}C , and ^{56}Fe , assuming $\sin^2 \theta_W = 0.2319$ and $n = 2$. It is readily seen that the relative importance of the recombination and bremsstrahlung neutrino processes increases as Z increases.

8. CONCLUDING REMARKS

We have summarized the results of the calculations of the neutrino energy-loss rates resulting from pair, photo-, plasma, bremsstrahlung, and recombination neutrino processes based on the Weinberg-Salam theory. A wide density-temperature regime $1 \leq \rho/\mu_e \leq 10^{14} \text{ g cm}^{-3}$ and $10^7 \leq T \leq 10^{11} \text{ K}$ has been considered. Extensive numerical tables for the pair, photo-, and plasma neutrino processes, FORTRAN programs for the interpolation formulae of the tables and for the analytic fitting formulae, and the text of this paper are published in computer-readable form in the AAS CD-ROM Series, Vol. 5. It is hoped that this paper will meet the needs of the researchers who wish to use the present results in their studies of stellar structure and stellar evolution.

We thank Achim Weiss, our referee, for a number of important suggestions regarding the improvement of the paper.

REFERENCES

- Beaudet, G., Petrosian, V., & Salpeter, E. E. 1967, *ApJ*, 150, 979
 Braaten, E. 1991, *Phys. Rev. Lett.*, 66, 1655
 Braaten, E., & Segel, D. 1993, *Phys. Rev.*, D48, 1478
 Dicus, D. A. 1973, *Phys. Rev.*, D6, 941
 Dicus, D. A., Kolb, E. W., Schramm, D. N., & Tubbs, D. L. 1976, *ApJ*, 210, 481
 Haft, M., Raffelt, G., & Weiss, A. 1994, *ApJ*, 425, 222
 Itoh, N., Adachi, T., Nakagawa, M., Kohyama, Y., & Munakata, H. 1989, *ApJ*, 339, 354; erratum 360, 741 (1990)
 Itoh, N., & Kohyama, Y. 1983, *ApJ*, 275, 858
 Itoh, N., Kohyama, Y., Matsumoto, N., & Seki, M. 1984a, *ApJ*, 280, 787; erratum 404, 418 (1993)
 ———. 1984b, *ApJ*, 285, 304; erratum 322, 584 (1987)
 Itoh, N., Kojo, K., & Nakagawa, M. 1990, *ApJS*, 74, 291
 Itoh, N., Matsumoto, N., Seki, M., & Kohyama, Y. 1984c, *ApJ*, 279, 413
 Itoh, N., Mutoh, H., Hikita, A., & Kohyama, Y. 1992, *ApJ*, 395, 622; erratum 404, 418 (1993)
 Jancovici, B. 1962, *Nuovo Cimento*, 25, 428
 Kohyama, Y., Itoh, N., & Munakata, H. 1986, *ApJ*, 310, 815
 Kohyama, Y., Itoh, N., Obama, A., & Hayashi, H. 1994, *ApJ*, 431, 761
 Kohyama, Y., Itoh, N., Obama, A., & Mutoh, H. 1993, *ApJ*, 415, 267
 Munakata, H., Kohyama, Y., & Itoh, N. 1985, *ApJ*, 296, 197; erratum 304, 580 (1986)
 ———. 1987, *ApJ*, 316, 708
 Ogata, S., & Ichimaru, S. 1987, *Phys. Rev.*, A36, 5451
 Pethick, C. J., & Thorsson, V. 1994, *Phys. Rev. Lett.*, 72, 1964
 Pinaev, V. S. 1964, *Soviet Phys.-JETP*, 18, 377
 Salam, A. 1968, in *Elementary Particle Physics*, ed. N. Svartholm (Stockholm: Almqvist and Wiksells), 367
 Schinder, P. J., Schramm, D. N., Wiita, P. J., Margolis, S. H., & Tubbs, D. L. 1987, *ApJ*, 313, 531
 Weinberg, S. 1967, *Phys. Rev. Lett.*, 19, 1264